ChemComm

Accepted Manuscript

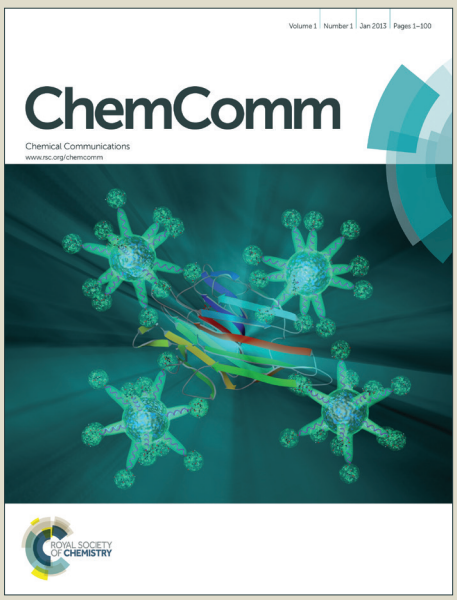

ROYAL SOCIETY OF CHEMISTRY

www.rsc.org/chemcomm

Journal Name

RSCPublishing

COMMUNICATION

Direct access to macroporous chromium nitride and chromium titanium nitride with inverse opal structure

Cite this: DOI: 10.1039/xoxxoooooox

Weitian Zhao[a] and Francis J. DiSalvo[b]

Received ooth January 2012,
Accepted ooth January 2012

DOI: 10.1039/xoxxoooooox

www.rsc.org/

We report a facile synthesis of single-phase, nanocrystalline macroporous chromium nitride and chromium titanium nitride with an inverse opal morphology. The material is characterized using XRD, SEM, HR-TEM/STEM, TGA and XPS. Interconversion of macroporous CrN to Cr_2O_3 and back to CrN while retaining the inverse opal morphology is also demonstrated.

Recent studies revealed the potential of transition metal nitrides as high performance catalyst supports, such as in proton exchange membrane fuel cell (PEMFC) applications.[1] The good electrical conductivity, high corrosion resistance and electrochemical stability of many transition metal nitrides may give them an advantage over conventional carbon or carbon-based materials, which suffer from long-term corrosion problems.[2,3] In addition, nitrides with catalytic activities that resemble noble metals have been reported, further increasing their potential as excellent candidates for catalyst support materials.[4]

For applications as catalyst supports, materials with high surface area which maximize the contact of catalyst with the fuels are desired. However, traditional bulk synthesis of nitride materials typically involves high temperature (above 800°C) and/or high-pressure, which causes significant sintering and produces products with large particle size and low surface area, thus do not meet the requirements for high-performance catalyst support.[5] Many efforts have been made to develop a low-temperature synthesis of nanocrystalline nitrides.[6] In addition to the particle size requirement, interest has been given to making an ordered porous structure. The ammonolysis (heating under flowing ammonia) of oxides is a common route in making nanostructured crystalline nitrides.[7,8] However, several problems and limitations are associated with this method. a) Oxides tend to sinter easily, making it a challenge to obtain oxides with nano-scale porous morphology. Some literature reports synthesis employing hard templates such as silica or carbon to keep the porous oxide from collapsing, but these templates can be difficult to remove later.[7,9] Besides, maintaining the morphology during nitridation of the porous oxide is a challenge as the conversion temperature of the thermodynamically favored oxide is reported to be generally very high.[10,11] In addition, the volume shrinkage upon nitridation may also contribute to the collapse of the pores. b) Ammonolysis of early transition metal oxides above 500°C produces nitrides with the rock salt structure. However, up to 10% oxygen impurities can present. Such impurities are reduced by processing at higher temperatures, which may again lead to changes in morphology. c) It is difficult to produce mixed metal nitrides of different stoichiometries as oxide precursors with a variable metal stoichiometry are generally not available, thus greatly limiting the applicability of that method.

For above reasons, it is desirable to achieve nitride formation without using an oxide intermediate. Hector *et al.* developed a nitride sol-gel process which employs metal dialkylamides $M(NMe_2)_n$ as nitride precursors.[12] By operating in air-free conditions, they were able to eliminate oxygen contamination in the synthesis. Specifically for TiN, the transamination of $Ti(NMe_2)_4$ with primary amines results in primary amide groups which can self-condense and form alkylimide bridges. By annealing of this dip-coated sol-gel film under ammonia, a nanocrystalline TiN film was obtained.[13] In their later work, they applied this method in synthesizing macroporous TiN and Ta_3N_5 by polystyrene template infiltration.[14,15] They also showed that the attempt to convert macroporous TiO_2 led to collapse of the pores. Despite the success of this method, extensive efforts are required for handling very air-sensitive precursors. In fact, Kaskel *et al.* demonstrated a facile approach in synthesizing high surface area titanium nitride by ammonolysis of $TiCl_4$ complexes.[16] This inspired our study of using metal chloride complexes as precursors to synthesize templated morphologies.

In this report, we focus on the synthesis and develop a facile method to fabricate nanocrystalline, ordered macroporous chromium nitride (CrN) through a template method using functionalized polystyrene (PS) beads. This method was further extended to fabricate mixed metal nitrides such as chromium titanium nitride ($Cr_{0.5}Ti_{0.5}N$). Both materials have been shown in earlier reports to be excellent catalyst supports for electrooxidation reactions in PEMFC anode. [1,17]

Macroporous CrN was synthesized by infiltrating pre-assembled PS beads followed by drying and nitridation under flowing ammonia at 450°C. Detailed procedures are described in the supporting information. Several samples were prepared by the same experimental procedure and the results were similar for all. The powder X-ray diffraction pattern for CrN nanoparticles (Figure 1) can be indexed well with the expected face-centered cubic phase of bulk chromium nitride. The blue lines are the peak positions of pure CrN with lattice parameter of 4.140 Å (PDF No. 04-007-9961). From the spectrum, the peaks are very broad and have narrow tips. This indicates nanoscale crystal domains with a relatively broad distribution of domain sizes. The average CrN crystal domain size is calculated to be 4.7 ± 0.8 nm using Halder-Wagner method. The lattice parameter was calculated to be a = 4.138 (12) Å using Whole Powder Pattern Fitting (WPPF) technique, giving a value which is very close to the reference data for CrN of 4.140 Å.

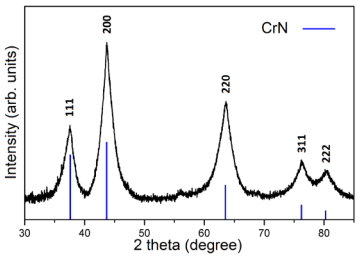

Fig.1 X-ray diffraction pattern of macroporous CrN.

Figure 2 is an SEM image showing the morphology of the macroporous CrN. For applications such as fuel cell support, the interconnected pores seen in the product will help facilitate effective flow of gases or liquids during operation. From the image, some surface inhomogeneities can be seen. This is likely due to residual precursors on the surface of the sample made by infiltration.

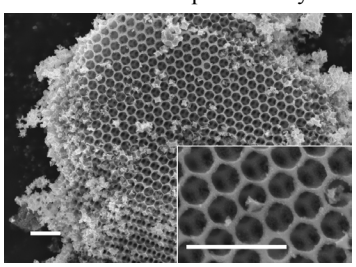

Fig. 2 SEM image of as-made CrN. Scale bars are 1 micron.

To investigate possible carbon content in the sample from PS decomposition, thermogravimetric analysis (TGA) was carried out in air. The change of weight and its derivative as a function of time are shown in Figure 3. The temperature profile is shown by the dashed line. Due to the release of species absorbed in air, such as water, a mass decrease before 120°C is observed in the raw data. The sample weight at 120°C is set as reference weight and only weight data after 120°C is shown. Two stages of weight increase as well as an obvious drop of weight can be observed from the image. The drop of weight is likely due to the oxidation of residual carbon to gaseous CO_2 in the sample, and the increase of weight is due to the oxidation of chromium nitride (CrN) to chromium oxide (Cr_2O_3), which is confirmed by XRD (Figure S1). From the TGA curves, it can be concluded that the carbon oxidation starts near 400°C and is completed near 480°C. In contrast, the oxidation of the CrN begins at a lower temperature (about 120°C) but is only nearly complete after 90 minutes at 550°C. The loss in weight from the peak at ~410°C to the minimum at ~480°C is about 5% of the material's weight, which can be a rough estimate of the carbon content in the material. The presence of amorphous carbon from PS decomposition is also reported in literature.[18]

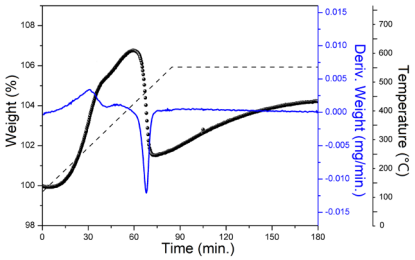

Fig. 3 TGA thermogram of macroporous CrN. Black dots are the measured data of sample weight. The continuous blue line indicates the derivative of the weight. The temperature profile is given in the dashed line.

The surface chemical states of the nitrides were probed using XPS. Survey scans and high-resolution scans were performed. Elemental composition was determined from peak area calculations and is listed in Table S1. The usage of sticky carbon tape for loading the sample during measurement and adventitious carbon make it difficult to determine the carbon and oxygen content from the data. A small amount of residual chlorine is also detected. The chromium nitrogen ratio was determined to be very close to 1:1. High-resolution XPS scans for N (1s) and Cr (2p) are shown in Figure 4.

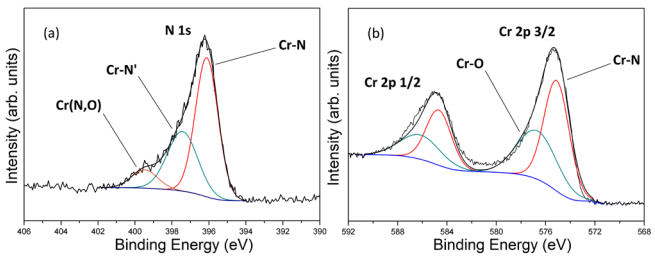

Fig. 4 Profiles of N 1s (a) and Cr 2p (b) from XPS high-resolution measurement. The fitting curve is given in black lines and the background in blue lines.

The nitride sample is conductive so the data is not calibrated by the standard carbon peak position. The measured data is deconvoluted and peaks are assigned to different chemical states according to reference data.[19] The Cr 2p 1/2 was also used in peak deconvolution. In the N 1s spectrum, major components of the peaks are contributed by the Cr-N bonds (396.1 eV, 397.4 eV) and perhaps a low level of oxynitride (399.5 eV). The two different states for CrN might be explained by complex environment around the atom due to oxygen impurities or defects in the structure. From the Cr 2p profile, two peaks at the position of 575.1eV and 576.7 eV are found. The first is assigned to CrN (575.8 eV) and the later falls into the region of CrO_x (576.3 – 579.8 eV).[19,20] The formation of a very thin surface oxide layer upon exposure to air is expected in nitride materials.

Ternary/mixed metal nitrides are generally difficult to make due to differences in activities and properties of the two different elements and their precursors. Never the less, we were able to expand the method to ternary metal nitrides to make nanocrystalline, macroporous $Cr_{0.5}Ti_{0.5}N$. The experimental details are given in the supporting information. It should be noted that it is also possible to make chromium titanium nitrides with other stoichiometries simply by varying the ratio between Cr and Ti precursors used, as no volatile species of Cr as well as Ti during synthesis are found. The molar ratio of metals in $Cr_{0.5}Ti_{0.5}N$ is later confirmed by high resolution EDX studies.

Figure 5 shows the powder X-ray diffraction pattern of macroporous $Cr_{0.5}Ti_{0.5}N$. The peaks can be indexed on a single face-centered cubic cell. The broad peaks indicate a small average crystal domain size, which is calculated to be 4.0 ± 0.7 nm. The weak peaks marked with an asterisk are background peaks from the sample holder.

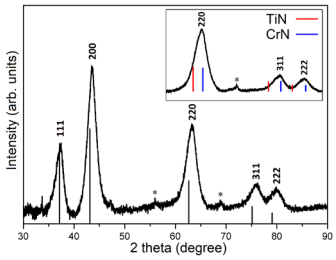

Fig. 5 XRD pattern of macroporous $Cr_{0.5}Ti_{0.5}N$ product.

The black lines correspond to a reported PDF card of a face-centered cubic $Cr_{0.5}Ti_{0.5}N$ with a lattice parameter of 4.192 Å (PDF no. 04-016-6620). The reported data also matches the expected value of 4.188 Å, assuming the lattice parameter of a $Cr_{0.5}Ti_{0.5}N$ solid solution follows Vegard's law, and thus is adopted as reference value. From WPPF, the lattice parameter of the product is calculated to be: a = 4.1569 (10) Å. A shift in peak positions from the PDF data, which is more obvious at higher angles, is observed in the spectrum. The formation of an oxynitride or carbonitride, as well as defects due to nitrogen vacancies $MN_x\square_{-x}$ will cause a shift in the lattice parameters and the resulting peak positions. Carbonitride formation from solid state synthesis, which will likely cause a peak position shift to lower angles due to larger carbon atoms, is unlikely to happen under the current experimental conditions as higher temperatures are often needed.[21] Defect structure and oxynitride formation decrease the lattice constant and shift the peak position to higher angles. The possible oxygen impurities in the samples are discussed later.

Another question here is whether the product is a $Cr_{0.5}Ti_{0.5}N$ solid solution, or a mechanical mixture of CrN and TiN. Since the lattice parameters of CrN and TiN are very close, lower-angle peaks are not sufficient to distinguish a single-phase product with a mixture that shows only one peak but contains two distinct peaks that are very close to each other. To prove the product is a solid solution, repeated measurements were conducted on higher-angle peaks. The spectrum, as well as the standard reference peak positions for CrN and TiN are shown in Figure 5 inset. The difference in the peak position from those expected for CrN and TiN is obvious at high angles. Since the line width is on the order of the difference between the bulk TiN and CrN peak position, a mixture of two products will result in a peak with a nearly flat top, which is not seen in the measured pattern. This suggests that the product is not a mixture of CrN and TiN. The inverse opal morphology with ordered interconnected pores of the $Cr_{0.5}Ti_{0.5}N$ is confirmed by SEM.

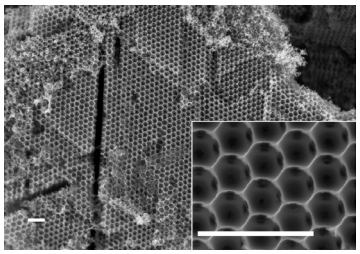

Fig. 6 SEM image of $Cr_{0.5}Ti_{0.5}N$. Scale bars are 1 micron.

An EDX study of elemental distribution was carried out using HR-STEM. Figure 7 is a High-Angle Angular Dark Field (HAADF) image of the macroporous $Cr_{0.5}Ti_{0.5}N$. A line scan was conducted and the path is shown as the yellow line in the figure. Concentrations of Cr and Ti are indicated by different colors. It was observed that the elemental concentration corresponds well with the thickness of the wall, and the Cr/Ti ratio is constant throughout this path, despite some possible instrumental errors. With a resolution of a few nanometers, these results show that chromium and titanium are reasonably well mixed. This is a further evidence for the formation of a CrN-TiN solid solution ($Cr_{0.5}Ti_{0.5}N$).

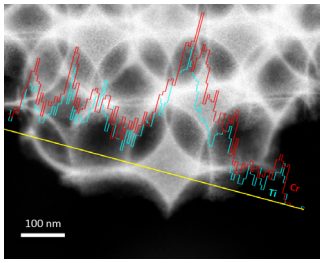

Fig. 7 HAADF image of macroporous $Cr_{0.5}Ti_{0.5}N$ and EDX line spectra indicating elemental concentration of Cr and Ti.

The elemental composition of $Cr_{0.5}Ti_{0.5}N$ determined by XPS is given in Table S1. As can be seen, Cl is no longer present in the material, possibly due to a higher annealing temperature. The Cr, Ti, N ratio is found to be 1:1.00:2.07, which is very close to the expected stoichiometry of $Cr_{0.5}Ti_{0.5}N$. Figure 8 shows the high-resolution analysis over Cr 2p and Ti 2p regions. Peak deconvolution gives two peaks for chromium, similar to the previous CrN sample. For titanium, two peaks at 456.0 eV and 457.5 eV were also identified. The first one can be assigned to TiN, but the second peak cannot be assigned according to reported values of Ti, TiO, TiN or TiO_2.[19] This peak falls in the region between TiN and TiO_2 and is hypothesized to be an oxynitride peak from a titanium atom connected to both nitrogen atoms and oxygen atoms. The results indicate that at the particle surface (first few nm), chromium mainly exists as CrN and titanium is mostly in the form of oxynitride.

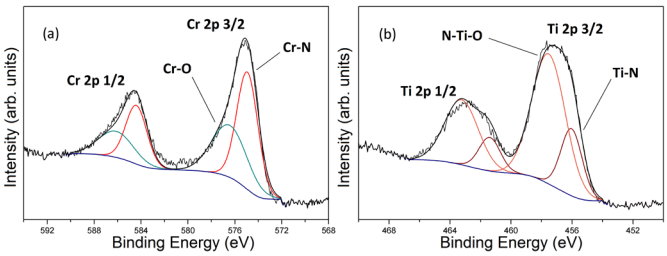

Fig. 8 Cr 2p profile (a) and Ti 2p profile (b) of macroporous $Cr_{0.5}Ti_{0.5}N$ measured in XPS.

To investigate the possible oxygen content in the sample. We synthesized $Cr_{0.5}Ti_{0.5}N$ nanoparticles without templates using different annealing temperatures (550°C and 800°C) and characterized them using a combustion analysis method, which can more accurately determine the oxygen and nitrogen content in the sample, as described in supporting information. The data shown in Table S2 shows that the sample annealed at 800°C is mostly nitride, while the sample annealed at 550°C has ~14 wt. % of oxygen impurities. However, this experiment cannot determine the exact cause for the peak shifting for the porous sample, which was shown in XPS to have a metal nitrogen ratio that matches the theoretical values expected for the nitride. Other factors such as vacancies in lattice could also result in peak position changes.

A possible conversion from macroporous CrN to Cr_2O_3 and then back to CrN was attempted in order to test on the thermal stability of the porous network during high temperature oxidation/nitridation. A similar interconversion of a Ti/W oxide and nitride was previously reported by our group.[22] For nitridation of Cr_2O_3 to CrN, previous work reported that an ammonolysis at 800°C for 8 h was finally able to completely eliminate the oxide phase.[10] It should be pointed out that the conversion temperature is dependent on oxide crystal size and/or any residual template materials in the sample. In fact, experiments in our lab showed a complete conversion to CrN with 6 hour ammonolysis at 650°C, from a macroporous Cr_2O_3 with a calculated crystal domain size of 24.9 ± 1.0 nm. Procedures to produce macroporous Cr_2O_3 from macroporous CrN and the nitridation process were described in detail in the supporting information.

Figure 9a shows the XRD patterns of all samples. Both converted materials showed a rock salt structure expected for CrN. However, for sample converted at 600°C, remaining Cr_2O_3 was found (data not shown). Figure 9b is an SEM image of the initial Cr_2O_3 made by oxidation of macroporous CrN in air at 550°C. While the porosity is still obvious, the details of the morphology appears mostly lost. A noticeable growth in particle size is also observed. Figure 9c and 9d are SEM images of the oxides that were re-nitrided by ammonolysis at 650°C and 700°C, respectively. The sample heated at 650°C exhibits an inverse opal morphology, while the sample heated at 700°C has mostly lost its original morphology. The pores within the sample provides open space for oxide growth, this might help maintain the porosity during conversion.

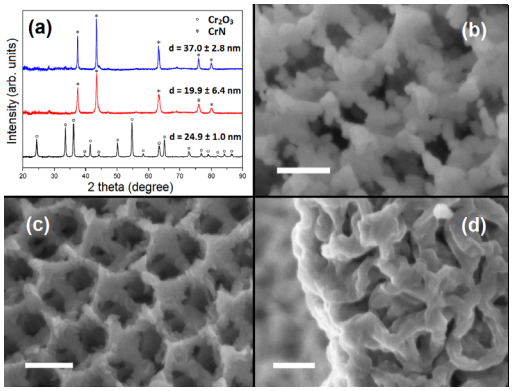

Fig. 9 XRD patterns and calculated crystal domain sizes of the initial macroporous Cr_2O_3 (black) and CrN obtained from ammonolysis at 650°C (red) or 700°C (blue) (a). SEM images of macroporous Cr_2O_3 (b) and CrN obtained from Cr_2O_3 heated at 650°C (c) and 700°C (d). Scale bars are 200 nm.

In this work, the conversion from macroporous oxide to nitride succeeded while preserving the porous morphology. However, the temperature window for successful conversion is very narrow (between 600°C - 700°C), and the crystal domain size of CrN grows to 20 nm compared to as-made CrN with d = 5 nm. This is likely due to the need of a higher temperature for a complete substitution of oxygen atoms by nitrogen atoms during the conversion process. In contrast, a direct nitride synthesis which can produce smaller crystals and is not restricted by nitridation temperature thus shows superiority. In this work, experiments were also conducted trying to obtain macroporous Cr_2O_3 directly from a PS bead template. Although we lowered the temperature to 400°C (the decomposition of PS is found to be between 300°C and 400°C as shown in Figure S2) and annealing time to 1.5 h, we were still not able to obtain good morphology due to large crystallite growth (calculated domain size ~ 35 nm). A typical SEM image of the samples obtained from this method is shown in Figure S3. This is a major reason that many reports of producing macroporous oxides involve the use of hard templates to suppress the crystal growth.

Besides the ability to produce nitrides directly from chloride complex precursors, this method also shows great potential in producing mixed metal nitrides in any stoichiometric ratio, which is difficult for the common oxide route. In fact, besides $Cr_{0.5}Ti_{0.5}N$, single phase, macroporous $Cr_{0.5}V_{0.5}N$ can also be made using this method. The crystalline phase and the morphology are confirmed by XRD and SEM, shown in supporting information, Figure S4 and Figure S5.

Conclusions

In summary, syntheses of macroporous CrN and $Cr_{0.5}Ti_{0.5}N$ from metal chloride complexes were demonstrated. The CrN product is a crystalline macroporous material with a crystal domain size of about 5 nm. A small amount of carbon (~5 wt. %) is estimated to exist in the final product. The chemical state of chromium was shown to be mostly chromium nitride by XPS. This synthetic method is shown to be capable in making macroporous mixed metal nitride $Cr_{0.5}Ti_{0.5}N$. A single phase, face-centered cubic structure chromium titanium nitride was obtained. The product is hypothesized to be a solid solution, instead of a mechanical mixture of CrN and TiN. Surface analysis by XPS reveals that Cr mostly exists in the nitride form with minor oxide, and Ti exists mainly in oxynitride state with some TiN. Slight peak position shift from reference data was observed in XRD. Combined with elemental analysis, it is possible that some oxygen is present in the sample prepared using this method. Interconversion of CrN to Cr_2O_3 and back to CrN while retaining the inverse opal morphology was also demonstrated. However, changes in morphology can be observed. The method of using common metal salts to directly obtain templated (mixed metal) nitride was demonstrated. This method was shown to be highly versatile and might be integrated into other templating methods in making porous nitride materials.

Notes and references

[a] Powder Technology Laboratory (LTP), École Polytechnique Fédérale de Lausanne (EPFL), Lausanne, Switzerland

[b] Department of Chemistry and Chemical Biology, Cornell University, Ithaca, New York 14853, USA

† Electronic Supplementary Information (ESI) available: Xxx. See DOI: 10.1039/c000000x/

1. (a) M. Yang, Z. Cui and F. J. DiSalvo, *Phys. Chem. Chem. Phys.*, 2013, **15**, 1088. (b) M. Yang, Z. Cui and F. J. DiSalvo, *Phys. Chem. Chem. Phys.*, 2013, **15**, 7041. (c) M. Yang, R. Guarecuco and F. J. DiSalvo, *Chem. Mater.*, 2013, **25**, 1783. (d) Z. Cui, M. Yang, H. Chen, M. Zhao and F. J. DiSalvo, *ChemSusChem*, 2014, **7**, 3356.
2. S. T. Oyama, *The Chemistry of Transition Metal Carbides and Nitrides*, Springer, 1996.
3. Y. J. Wang, D. P. Wilkinson and J. Zhang, *Chem. Rev.*, 2011, **111**, 7625.
4. A. M. Alexander and J. S. J. Hargreaves, *Chem. Soc. Rev.*, 2010, **39**, 4388.
5. G. V. White, K. J. D. Mackenzie, I. W. M. Brown, M. E. Bowden and J. H. Johnston, *J. Mater. Sci.*, 1992, **27**, 4294.
6. B. Mazumder and A. L. Hector, *J. Mater. Chem.*, 2009, **19**, 4673.
7. Y. Shi, Y. Wan, R. Zhang and D. Zhao, *Adv. Funct. Mater.*, 2008, **18**, 2436.
8. M. Y. Tsang, N. E. Pridmore, L. J. Gillie, Y. H. Chou, R. Brydson and R. E. Douthwaite, *Adv. Mater.*, 2012, **24**, 3406.
9. E. Ramasamy, C. Jo, A. Anthonysamy, I. Jeong, J. K. Kim and J. Lee, *Chem. Mater.*, 2012, **24**, 1575.
10. Y. Li, L. Gao, J. Li and D. Yan, *J. Am. Ceram. Soc.*, 2002, **85**, 1294.
11. G. Mangamma, P. K. Ajikumar, R. Nithya, T. N. Sairam, V. K. Mittal, M. Kamruddin, S. Dash and a K. Tyagi, *J. Phys. D. Appl. Phys.*, 2007, **40**, 4597.
12. D. V. Baxter, M. H. Chisholm, G. J. Gama, V. F. Distasi, A. L. Hector and I. P. Parkin, *Chem. Mater.*, 1996, **8**, 1222.
13. A. W. Jackson and A. L. Hector, *J. Mater. Chem.*, 2007, **17**, 1016.
14. B. M. Gray, S. Hassan, A. L. Hector, A. Kalaji and B. Mazumder, *Chem. Mater.*, 2009, **21**, 4210.
15. C. F. Mallinson, B. M. Gray, A. L. Hector, M. A. Mclachlan and J. R. Owen, *Inorg. Chem.*, 2013, **52**, 9994.
16. S. Kaskel, K. Schlichte, G. Chaplais and M. Khanna, *J. Mater. Chem.*, 2003, **13**, 1496.
17. Z. Cui, M. Yang and F. J. Disalvo, *ACS Nano*, 2014, **8**, 6106.
18. M. C. Orilall, N. M. Abrams, J. Lee, F. J. Disalvo and U. Wiesner, *J. Am. Chem. Soc.*, 2008, **130**, 8882.
19. J. F. Moulder, W. F. Stickle, P. E. Sobol and K. D. Bomben, *Handbook of X-Ray Photoelectron Spectroscopy*, Perkin-Elmer Corporation (Physical Electronics), 1992.
20. A. Lippitz and T. Hübert, *Surf. Coatings Technol.*, 2005, **200**, 250.
21. C. Giordano, C. Erpen, W. Yao, B. Milke and M. Antonietti, *Chem. Mater.*, 2009, **21**, 5136.
22. C. V. Subban, I. C. Smith and F. J. Disalvo, *Small*, 2012, **8**, 2824.

